The Oxford Scanning Proton Microprobe

Jacqueline Koay and Geoffrey W. Grime
Scanning Proton Microprobe Unit, Nuclear Physics Laboratory, University of Oxford, Oxford, UK, OX1 3RH

The scanning proton microprobe uses a focused beam of MeV protons to give analytical information by exploiting two physical processes, particle induced X-ray emission (PIXE) and Rutherford Backscattering (RBS). Scanning transmission ion microscopy may also be included in the nuclear microscopy package to give imaging data. PIXE is particularly appropriate for biomedical research as signals from hydrogen, carbon, nitrogen and oxygen, which are the main components of a biological matrix, are not detected and therefore signals from inorganic elements with $z > 10$ will not be swamped by signals from the matrix. Elements with $z < 10$ can, however, be detected using RBS when present at higher concentrations.

Apart from the biomedical field, the SPM has wide-ranging applications spanning diverse areas such as archaeology, materials science and environmental chemistry. This paper reviews the theory of ion beam analysis, the Oxford Scanning Proton Microprobe and outlines some of the work currently being carried out at Oxford.

The Scanning Proton Microprobe (SPM)

The nuclear microprobe shares the same principles as the analytical electron microscope in that the sample is scanned by a focused beam of charged particles, but instead of keV electrons, MeV protons and light ions are used. This gives a number of advantages: firstly, the detection limits for PIXE are 2–3 orders of magnitude lower than for energy dispersive X-ray analysis (EDX), giving faster, more sensitive analysis; secondly, the beam will penetrate thick ($\leqslant$50 μm) samples with no loss of spatial resolution; and thirdly, other analytical techniques exploiting nuclear interactions [*e.g.*, Rutherford backscattering (RBS)] can be used to give additional analytical information.

This non-destructive method of identifying, localizing and quantifying elements in a matrix allows for re-analysis, achieving sensitivity at parts per million level using PIXE,[1] and the accuracy is such that elemental concentrations in a sample can be determined with a typical accuracy of 10%.

Analytical Techniques

When a beam of MeV ions impinges on a target, various reactions take place between the particles and the electrons and nuclei of the sample atoms (Fig. 1). Radiation or particles from these can be detected to give analytical information. The most important techniques for nuclear microscopy are particle induced X-ray emission (PIXE), Rutherford backscattering and scanning transmission ion microscopy (STIM).

Particle Induced X-ray Emission

The collision of projectile ions and the stationary atoms in the matrix results in a transfer of energy which, in turn, results in the ejection of an electron from the inner shell of the target atom. This vacancy is almost instantaneously filled by an electron from a higher energy state, resulting in the emission of an X-ray photon with an energy characteristic of the target atom. This proton can be detected using an energy dispersive detector to identify and quantify the elements in a matrix of unknown composition.

When using a lithium-drifted silicon (Si–Li) detector, PIXE is a multi-elemental technique, although absorption in the thin beryllium windows normally fitted to Si–Li detectors limits the detectable elements to $z \geqslant 12$. In addition, because PIXE is an inner-shell process, chemical binding and surface effects are negligible, and so the process can be described using simple models. This leads to an accuracy and reproducibility of 5–10% in most instances, with very little dependence on standards.

In thick samples, self-absorption corrections must be applied, but again, these are well understood and can be incorporated easily into the results using standard PIXE software, provided that the sample matrix is known.

The sensitivity of PIXE is superior to that of the electron probe because electron probes suffer from high background (Fig. 2). This high background is contributed by bremsstrahlung radiation. A particle has its own electric field, and when the particle changes its speed or direction rapidly, a shock wave in the electric field causes the emission of electromagnetic radiation. Protons are not deflected as much as electrons by electrons in the target atoms and, as a result, virtually no bremsstrahlung photons are emitted when protons are used as projectiles in comparison with an electron–electron collision. The low energy background in the proton PIXE spectra arises from secondary electron bremsstrahlung from the slowing down within the matrix of electrons which were ejected during the ionization process. This is much less intense than primary bremsstrahlung in the electron microprobe.

From Fig. 2 it can be seen that, unlike the electron microprobe, which is background limited, the sensitivity of the proton microprobe is statistics limited, and can be improved with counting time and by counting X-rays more efficiently, which is why PIXE requires the use of large-area detectors. Other factors that affect the sensitivity of micro-PIXE include

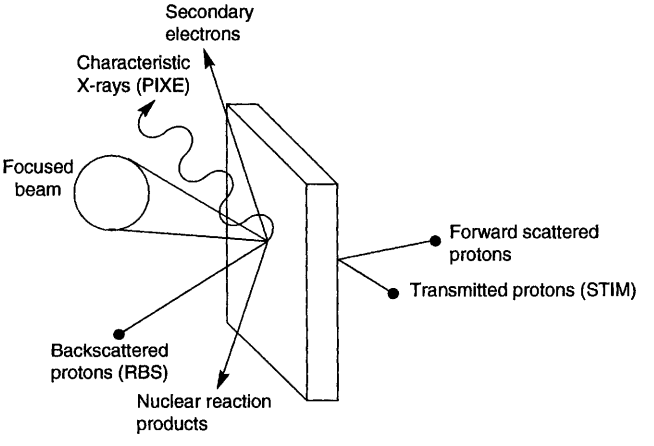

Fig. 1 Reactions between projectile ions and target atoms. A beam of monoenergetic particles is fired at the sample in a vacuum chamber

the proton energy used and the effects due to absorption or strong X-ray lines from major elements in the matrix.

Sensitivity can be expressed absolutely, in terms of mass, or relatively, in terms of mass per mass (or parts per million). Only taking into account SEB, the sensitivity of PIXE is typically 10^{-6} mass per mass, and is dependent upon factors such as beam current and data collecting time. The sensitivity can be further degraded by interferences occuring between light and heavy elements, as these lines occur in the same region of the energy spectrum. For an example, the $L(\beta)$ peak of cadmium ($E = 3.317$ eV) and the $K(\alpha)$ peak of potassium ($E = 3.314$ eV) overlap with each other. The overlap of $K(\alpha)$ and $K(\beta)$ peaks of neighbouring elements in the transition metal region is another example of this. Complex energy spectra can be unscrambled by the various spectrum fitting software packages that are now available.

Rutherford Backscattering

The backscattering phenomenon is observed when a small fraction of projectile ions from the incident beam approaches the target nuclei sufficiently closely to be scattered through an angle of $\theta \approx 180°$ from the incident beam by Coulombic repulsion. A two-body, elastic collision occurs (see Fig. 3).

The majority of particles passing through matter undergo small-angle collisions with electrons, causing them to lose energy and deviate from their trajectory slowly. Occasionally, a particle may have a direct collision with a nucleus and may recoil back out of the sample. Measurement of the energies of the recoiled particles yields analytical data on sample composition and thickness.

The energy loss of the projectile ion has two components: energy loss upon collision with the nuclei of target atoms and the energy loss the ion suffers as it traverses the matrix to the collision site. The quantity of energy lost by the recoiling ion from direct elastic collisions is proportional to the mass of the target nuclei (recoil from heavy nuclei having greater energy). Each element thus has its own depth coordinate sysem in the RBS spectrum which enables identification of elemental composition in an unknown matrix.

Fig. 4 shows the RBS spectrum of a biological matrix composed mainly of carbon, nitrogen and oxygen. Light elements, such as these which compose a typical biological matrix, can be characterized by RBS. The relative height of each 'step' is indicative of the empirical formula of the unknown matrix. The minimum detectable limit of RBS is approximately 1000 ppm.

RBS is thus able to perceive depth distribution of matrix atoms under the surface and yield quantitative composition data. The thickness of the matrix can also be measured by RBS and, together with the major element composition, be used to correct the data from PIXE measurements in thick samples. RBS gives an independent measure of accumulated charge, and these data can be used to correct experimental measurements, which are a source of inaccuracy in PIXE data.

Scanning Transmission Ion Microscopy

STIM represents the third aspect of nuclear microscopy which, when used in conjunction with PIXE and RBS, yields a complete picture of the sample under investigation. STIM could also stand on its own as a powerful imaging tool which complements scanning electron microscopy (SEM) results. Structures beneath the surface that are not visible by SEM can be imaged by STIM. However, STIM could not distinguish between a thick region of the sample or an inclusion in the matrix.

Sealock *et al.*[3] reported that imaging with STIM was superior to other similar techniques in terms of efficiency and spatial resolution.

STIM measures the energy of particles that pass through the sample (Fig. 5). (Thus, STIM is only applicable for samples with a thickness less than approximately 50 μm.) The loss of the projectile kinetic energy depends on the thickness, density and composition of the target at the beam location, as the energy loss is due to the collisions of the MeV projectile ions

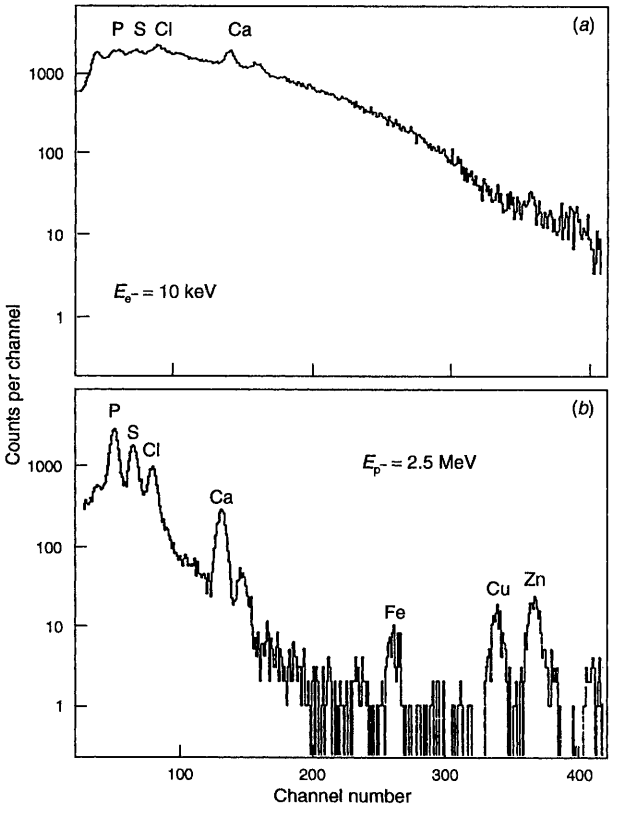

Fig. 2 Comparison of background from electron microprobe (*a*) and proton microprobe (*b*) (from K. Traxel in reference 2)

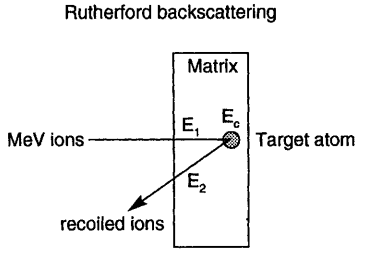

Fig. 3 Two body elastic collision (RBS). Energy loss from traversing the matrix = $E_1 + E_2$; energy loss from collision with target atom = E_c

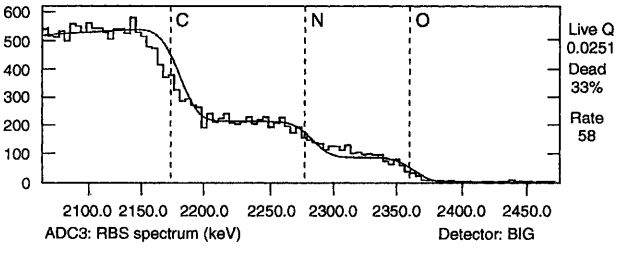

Fig. 4 An ABS spectrum of a biological matrix. The matrix is derived from an amyloid core found in cartilage tissues

with atomic electrons. The energy changes arising from these interactions can be used to image sample structure.

Fig. 6 shows an STIM image of an integrated circuit, with the contrast arising from additional thickness of the metallization layers. STIM is capable of achieving a resolution of 50 nm[4] and is therefore a suitable technique for analysing microelectronic devices which are continuously being decreased in size as technology progresses. The composition, thickness and distribution of buried layers in microcircuit structures can be imaged by STIM because of the penetrative powers of MeV protons.

Summary

Combining the three techniques in the nuclear microscopy package, namely PIXE, RBS and STIM, gives a very powerful imaging tool which is capable of: giving quantitative data with high precision and accuracy (PIXIE/RBS); elemental mapping (PIXE); characterizing unknown matrix composition (RBS); identifying pathological features in biological tissues characterized by density without the use of stains (STIM); and visualizing structures beneath the surface without the need to etch (STIM).

Oxford Microprobe

Hardware

The Oxford SPM[5] was established in its present form in 1987. Megaelectronvolt protons are generated by using a small tandem Van der Graff accelerator (Fig. 7). Negative hydrogen ions from a plasma source are injected into the low energy tube of the accelerator, where they are accelerated towards the positively-charged terminal, gaining 1.5 MeV in the process. At the positive terminal, the negative charge on the ions is stripped by nitrogen gas. The positive ions are then accelerated through the high energy tube to emerge as a beam of particles of energy $v(1 + q)$ MeV, where v is the voltage of the terminal in MV and q is the charge state of the ion. Thus, in the case of protons, the proton energy of the emergent beam is twice that at the terminal (3 MeV) and the ions have a velocity approximately one tenth of the speed of light (Fig. 7).

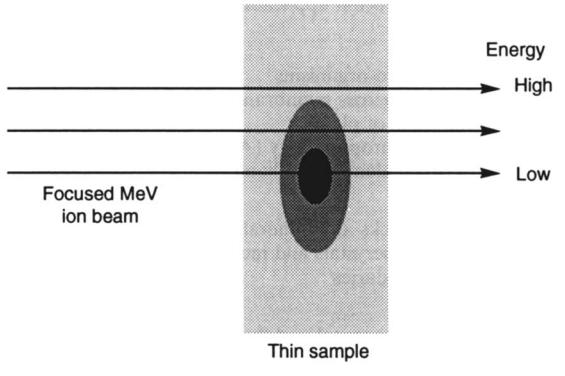

Fig. 5 STIM: measurement of the energy of transmitted particles

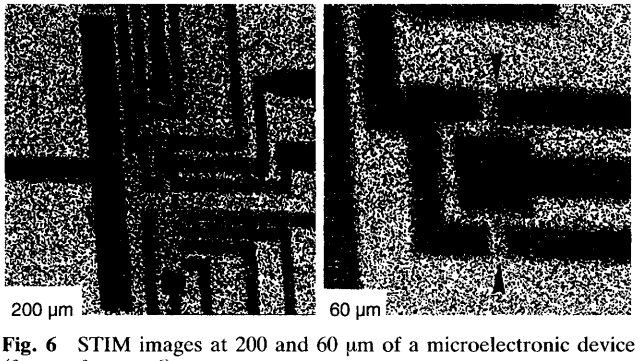

Fig. 6 STIM images at 200 and 60 μm of a microelectronic device (from reference 6)

The magnetic quadrupole lenses used at Oxford to focus the beam are the key part of the Oxford microprobe. Focusing the beam to the micron diameter requires new technology, as the cylindrically symmetrical lenses developed for electron microscopy do not possess sufficient force to focus a highly energetic, ion beam. Magnetic quadrupole lenses are more effective for use with heavier charged particles because the magnetic field lines are hyperbolic and normal to the direction of motion of the particles (Fig. 11), resulting in a strong force, $F = v \times B$, directed towards or away from the axis of the lens.

The action of a single quadrupole lens on the ion beam is such that the beam converges in one plane and diverges in another (Fig. 8). Thus, a minimum of two such lenses is required to focus a beam of charged particles simultaneously in two planes. At Oxford, a series of three quadrupole lenses is used (Fig. 9). The layout of the Oxford SPM is shown in Fig. 12. The spot size is limited by various abberations, due both to intrinsic effects in a perfect lens and also imperfections of construction and alignment, which also have the effect of degrading the image. At Oxford, a 1 μm diameter is routinely achieved and, following careful alignment of the lenses, a diameter of 0.4 μm has been achieved with currents sufficient for PIXE analysis.[6]

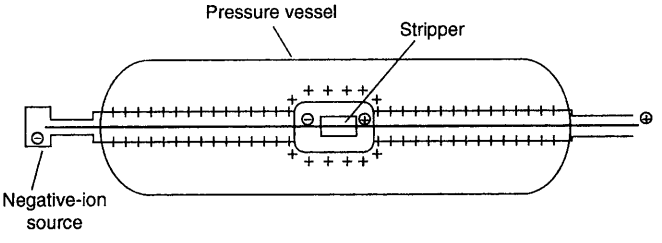

Fig. 7 Tandem electrostatic accelerator. The negative hydrogen ions are accelerated to the positive terminal, where the negative charge is stripped off the ion. The positive ion is now accelerated down the second tube, emerging with twice its original velocity

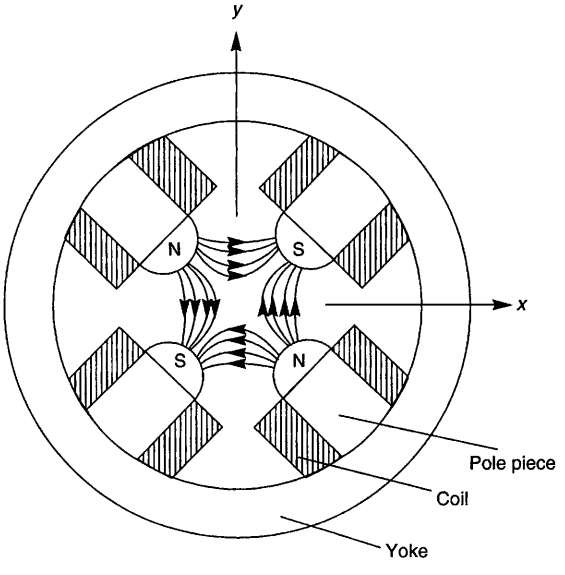

Fig. 8 The action of a quadrupole field on a charged particle. The arrows represent the direction of the magnetic field force on a charged particle passing down into the lens for various positions in the cross-section plane (from reference 8)

The focused beam is scanned over the target using magnetic coils and, for a 3 MeV proton beam, the maximum scanned area is 2.5 × 2.5 mm. Various detectors positioned strategically in the vacuum target chamber (Fig. 10) measure the events arising from the interaction between the proton beam and the component atoms in the sample. Data pulses are recorded together with the instantaneous beam position, and this can be used to construct elemental maps, one-dimensional line profiles or point concentration analyses of the sample. The data acquisition system incorporates a graphics workstation for operator interfacing and a mainframe computer for archiving and off-line data processing.

Applications of the Oxford Microprobe

A wide range of studies have been carried out using the Oxford Scanning Proton Microprobe (Table 1). This paper highlights some of the current research interests of the group (Table 2).

Defects in Crystals

Defect in crystals, such as stacking faults in a silicon crystal, can be studied by STIM. By use of this technique, a phenomenon called channelling can be studied. Channelling causes a reduction in the energy loss rate of ions passing through a crystalline material when the beam direction is aligned with the crystal axis, and this phenomenon enables the study of defects in the crystal structure.

Fig. 13(*a*) is an image of a stacking fault near the surface of a silicon crystal, taken using STIM. The 30 μm image is a map of the energy loss of 3 MeV protons transmitted through the silicon, which has a thickness of about 40 μm. The proton beam was channelled in the (110) plane of the crystal. The fault is visible because of the de-channelling it produced, causing some of the protons to be transmitted with a higher energy loss than if they had passed through a region of crystal with no fault.

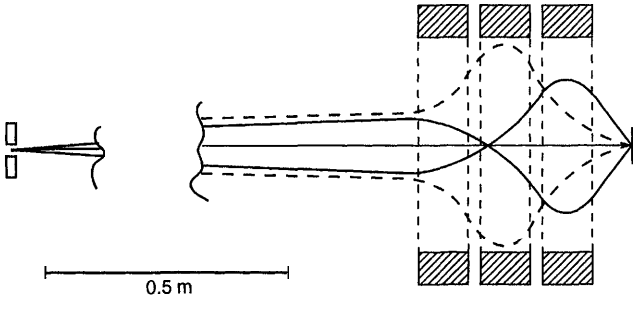

Fig. 9 Triplet configuration quadrupole lenses of the Oxford microprobe. Beam profiles in horizontal and vertical planes are indicated by solid and broken lines, respectively (from reference 2)

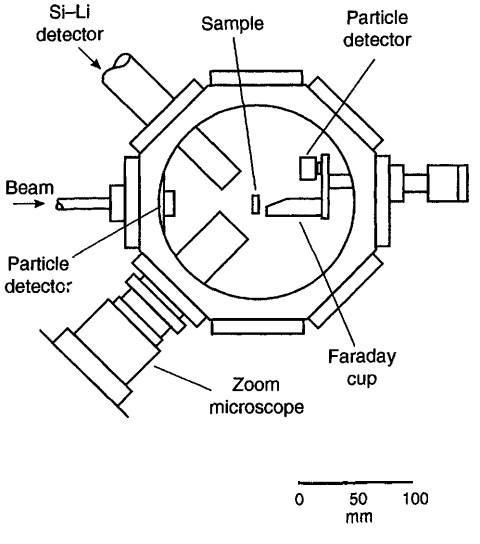

Fig. 10 Schematic plan view of the target chamber showing the arrangements for the zoom microscope, Si(Li) detector, RBS particle detector and the rotating mount holding the Faraday cup and the STIM particle detector (from reference 2)

Table 1 A summary of the capabilities of nuclear microscopy

Analysis
PIXIE: 1–10 ppm MDL for $z > 13$.
Multielemental
5–10% accuracy
RBS: 0.1–1% MDL
Optimum for $z < 10$
(light element stoichiometry)
Depth profiling

Spatial resolution
0.4 1 μm (PIXE, RBS)
0.1–0.2 μm (STIM, IBIC)
Maintained in thick samples

Imaging
STIM: Density mapping for thickness 1–30 μm
SEM: Surface topography mapping using secondary electrons
IBIC: Semiconductor device mapping using beam-induced charge
Tomography: 3-D imaging using STIM

Crystal studies (with channelling)
Defect imaging in thick (< 30 μm) samples
Lattice location of impurity atoms

Table 2 A summary of recent applications of the Oxford SPM

Life sciences
Metal uptake by micro-organisms
Elemental gradients across membranes
Defence mechanisms of plants
Trace elements in neuropathology (Alzheimer's disease, *etc.*)
Metal toxicity (toxic elements in hair)

Geosciences
Element zoning in rocks and minerals
Composition of microcrystals and inclusions
Studies of grain boundaries

Environmental sciences
Population studies of aerosol and fly-ash particles
Studies of lake sediment particles
Trace element distribution in lake sediment porewater
Biogeochemical weathering of rocks

Archaeometry
Studies of painting pigments
Studies of pigments in glasses and ceramics
Use–wear analysis of flint tools
Trace elements in buried bone

Materials science
Channelling studies of crystals (dislocation imaging, strain mapping)
Mapping complex devices with IBIC
STIM mapping of multi-layer devices
Fabrication on high aspect ratio structures in photoresist

Industrial
Metal diffusion in polymers
Electrode surface studies
Chemical effects in catalysts

Paracetomol-induced Toxicity in Rat-liver Cells

Normal cells maintain a sodium–potassium gradient across the cell membrane. The high sodium–low potassium concentration within a cell is present due to the action of biological pumps which are powered by ATP. Toxins affect the functioning of these pumps and induce a variety of biochemical reactions, which could be quantified by using the scanning proton microprobe. The SPM is particularly suited to biological applications, as using STIM precludes the need for staining, and cells can be studied in a state as close as possible to their *in vivo* state. Figure 13(*b*) shows a section of rat liver tissue, unstained and cryofixed with liquid nitrogen. Cell boundaries and sinusoidal spaces are visible from the potassium and phosphorus PIXE maps [Fig. 13(*b*)].

Bivalves as Environmental Monitors

Bivalves, such as mussels, grow in a process called accretion, where successive layers of shell are laid down in a similar pattern to roofing tiles. The shell material is predominantly calcium carbonate, with a small fraction of organic material. The chemistry of the environment strongly affects the composition of the skeleton, as trace elements are incorporated into the shell material during the growth process. Bivalves and corals also exhibit banding patterns [Fig. 13(*c*)] as a function of time, and quantitative analysis of the mussel shell with reference to the banding pattern may provide a record of water quality and other environmental conditions in the local environment of the organism over a period of time.[8,9] Fig. 13(*c*) shows calcium and strontium PIXE maps of a mussel shell from the Conwy. Note that the distribution of calcium is uniform, whilst the strontium map shows a banding pattern that is indicative of the age of the organism.[10] Work is currently being carried out in collaboration with the Department of Environmental and Evolutionary Biology of Liverpool University to age mussel shells and fish otoliths using PIXE.

Line scans across the mussel shell indicate the variability in elemental composition as a function of distance (hence time).

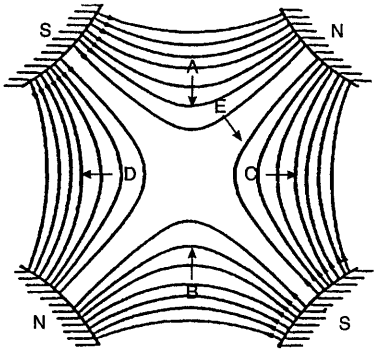

Fig. 11 The direction of motion of a charged particle in a magnetic field

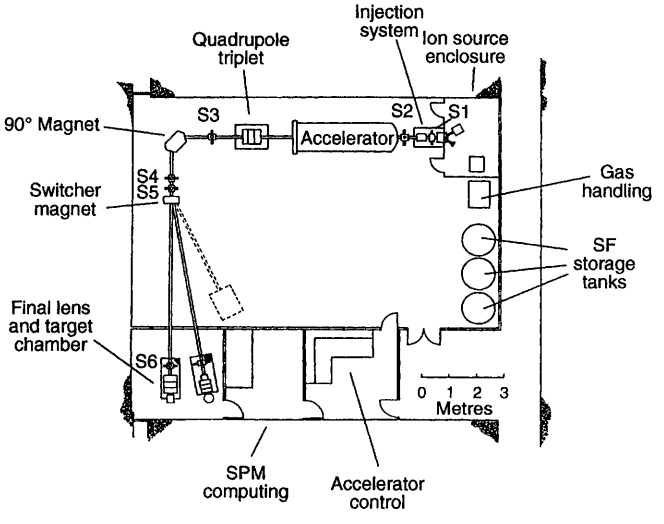

Fig. 12 Plan of the layout of the SPM facility

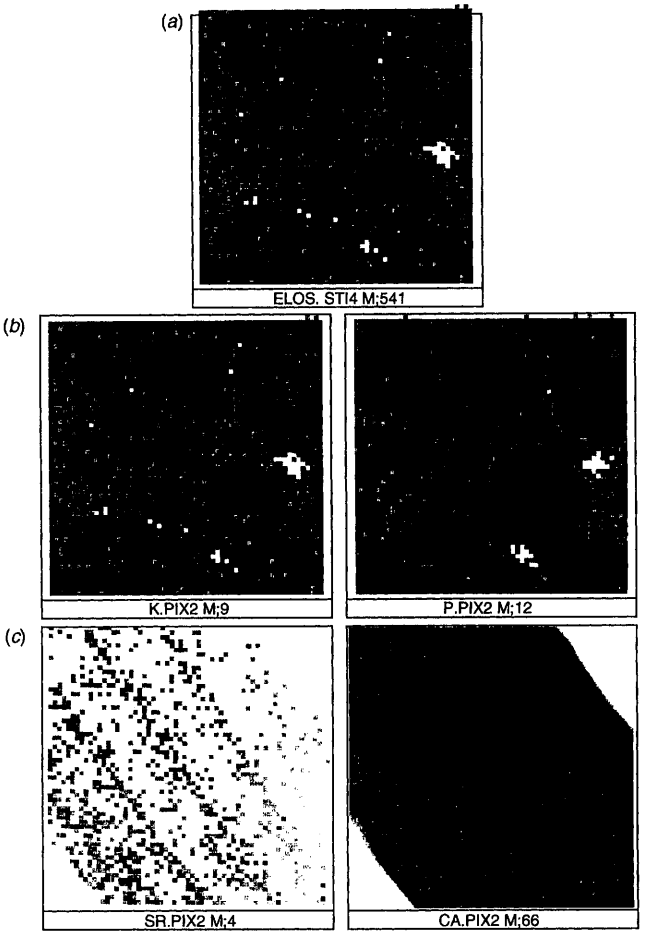

Fig. 13 (*a*), STIM image of a silicon crystal (30 μm) (from reference 12); (*b*), rat liver tissues: potassium and phosphorus PIXE maps at 500 μm; (*c*), mussel shell: strontium and calcium PIXE maps at 1500 μm

References

1 Johansson, T. B., Akelsson, R., and Johansson, S. A. E., *Nucl. Instr. Meth.*, 1970, **84**, 141.
2 *Principles and Applications of High-energy Ion Microbeams*, eds. Grime, G. W., and Watt, F., Adam Hilger, Bristol, 1987.
3 Sealock, R. M., Jamieson, D. N., and Legge, G. J. F., *Nucl. Instr. Meth.*, 1987, **B29**, 557.
4 Bench, G. S., and Legge, G. J. F., *Nucl. Instrum. Meth.*, 1989, **B40/41**, 655.
5 Grime, G. W., 'Nuclear Microscopy—A novel Technique for Material Characterisation', *Inst. Phys. Conf. Ser. No. 130*, 1992, Ch. 2.
6 Breese, M. B. H., Grime, G. W., and Watt, F., *Annu. Rev. Nucl. Part. Sci.*, 1992, **42**, 1.
7 Grime, G. W., and Watt, F., *Nucl. Instr. Meth.*, 1993, **B75**, 495.

8 Grime, G. W., and Watt, F., *Beam Optics of Quadrupole Probe-forming Systems,* Adam Hilger, Bristol, 1984.
9 Swann, C. P., Carriker, M. R., and Ewart, J. W., *Nucl. Instr. Meth.*, 1984, **B3**, 392.
10 Lindh, U., Mutvei, H., Sunde, T., and Westermark, T., *Nucl. Instr. Meth.*, 1988, **B30**, 388.
11 Coote, G. E., and Trompetter, W. J., *Nucl. Instr. Meth.*, 1993, **B77**, 501.
12 King, P. J. C., Bresse, M. B. H., Wilshaw, P. R., Booker, G. R., Grime, G. W., Watt, F., and Goringe, M.J., *Inst. Phys. Conf. Ser. No. 134: Sect. 3*, 1993.

Paper 4/02788D
Received May 11, 1994
Acceptd May 12, 1994